Optimal design of PV-based grid-connected hydrogen production systems

Journal of Cleaner Production 434 (2024) 140007

Contents lists available at ScienceDirect

Journal of Cleaner Production

journal homepage: www.elsevier.com/locate/jclepro

Optimal design of PV-based grid-connected hydrogen production systems

Paolo Marocco *, Marta Gandiglio, Massimo Santarelli

Department of Energy, Politecnico di Torino, Corso Duca degli Abruzzi 24, 10129, Torino, Italy

ARTICLE INFO

Handling Editor: Jin-Kuk Kim

Keywords:
Power-to-hydrogen
Hydrogen
Electrolysis
Solar energy
Optimal design
Decarbonisation

ABSTRACT

A cost-optimal design of power-to-hydrogen (PtH) systems is crucial to produce hydrogen at the lowest specific cost. New challenges arise when it comes to ensuring a reliable and cost-effective hydrogen supply in the presence of variable renewable energy sources. In this context, the aim of this analysis is to investigate the optimal design of PV-based grid-connected hydrogen production systems under different scenarios. To this end, an optimisation framework based on the mixed integer linear programming (MILP) technique is developed. Results are presented by employing a set of techno-economic and environmental indicators to provide general guidance on how to optimally size PtH systems, going beyond the analysis of a specific case study. The analysis is applied to Italy and particular attention is paid to exploring the impact of the price of grid electricity.

The results indicate that the price of grid electricity strongly affects the optimal design of PtH systems. Specifically, in scenarios with high electricity prices, it is economically convenient to significantly oversize the PV plant and the electrolyser. The optimal PV ratio, representing the ratio between the PV size and the electrolyser size, increases from 1.6 to 2.7 as the electricity price rises from 50 to 300 €/MWh. Additionally, when electricity prices exceed approximately 120 €/MWh, the optimal electrolyser size (in terms of hydrogen production under rated conditions) becomes almost three times larger than the average hydrogen demand. By comparing grid-connected and off-grid scenarios, the importance of the electrical grid is also highlighted: even when poorly used, it plays a crucial role in limiting the size of the hydrogen storage. The levelised cost of hydrogen for the optimal PtH configuration falls within the range of 3.5–7 €/kg (depending on the price of grid electricity) and increases to 8.2 €/kg when the system operates off-grid. Finally, the hydrogen carbon footprint, quantified as $kg_{CO2,e}/kg_{H2}$, is also explored. Considering the current price and carbon intensity of grid electricity, the cost-optimal PtH configuration already involves the production of renewable hydrogen (<3 $kg_{CO2,e}/kg_{H2}$).

1. Introduction

Hydrogen is currently experiencing an unprecedented momentum, and the number of hydrogen-related policies and projects around the word is growing rapidly. Hydrogen is indeed expected to play a key role in accelerating the transition towards a carbon neutral future (van der Spek et al., 2022). At present, it is used as a feedstock for chemical production (e.g. ammonia and methanol), as a reducing agent in the steel industry and to remove impurities and upgrade heavy oil fractions in refineries (IEA and Global, 2022). Moreover, in a decarbonised society, hydrogen – and hydrogen-derived fuels – will cover a wide range of end uses: applications where high energy density is crucial (e.g. shipping and aviation), the chemical industry and the storage of energy over long periods of time (Mertens et al., 2023).

1.1. Hydrogen for the decarbonisation of end-use sectors

Massaro et al. (2023) discussed the potential and technical challenges of the use of hydrogen for a zero-emission aviation. Due to the low energy density of batteries, hydrogen will be necessary to pursue all-electric aviation in the coming years. However, improvements (e.g. in terms of weight) are needed for both hydrogen storage and fuel cell technologies to make the hydrogen-based solution technically feasible for aircraft electrification. In addition, the use of hydrogen in combination with fuel cells is highly suited for heavy vehicles travelling over long distances (e.g. trucks and regional/intercity buses) (IRENA, 2018). However, relevant obstacles still need to be overcome, such as costly investments, limited adequate infrastructure and the lack of defined norms and standards (Genovese et al., 2023). As shown within the framework of the REMOTE project, hydrogen is also essential to provide long-term energy storage in scenarios with high penetration of

* Corresponding author.
E-mail address: paolo.marocco@polito.it (P. Marocco).

https://doi.org/10.1016/j.jclepro.2023.140007
Received 9 October 2023; Received in revised form 22 November 2023; Accepted 27 November 2023
Available online 2 December 2023

renewable energy sources (RES) (Bionaz et al., 2022; Gandiglio et al., 2022). Hydrogen-based energy storage, indeed, becomes crucial to achieve a cost-effective system configuration in 100% renewable energy systems since it avoids oversizing RES generators and batteries (Marocco et al., 2023a). As for industrial applications, hydrogen is considered a key pillar for the decarbonisation of the steel sector: it can be used as a primary reducing agent in the Direct Reduced Iron (DRI) process and as a secondary reducing agent in the Blast Furnace-Basic Oxygen Furnace (BF-BOF) process. Hydrogen can also constitute a promising solution to produce high-temperature heat, which is currently mainly supplied by the combustion of fossil fuels (Marocco et al., 2023b). As reported by IRENA (IRENA, 2022a), decarbonising high-grade heat through hydrogen can be preferable and less invasive compared to an alternative route based on electrification.

It should be stressed that hydrogen must be produced sustainably to comply with the long-term decarbonisation targets. However, today's hydrogen production is almost entirely based on natural gas and coal (grey hydrogen), which together account for more than 95% of the global hydrogen production (IRENA, 2021). Therefore, a shift towards low-carbon hydrogen production pathways needs to take place, also coping with the sharp increase in hydrogen demand foreseen in the coming years (Zainal et al., 2023). The total hydrogen production is expected to exceed 600 Mt per year in 2050, accounting for about 12% of the final energy use (IRENA, 2022b). Although currently expensive, the competitiveness of green hydrogen is improving due to the rapidly falling costs of renewable electricity. In the period from 2010 to 2021, the investment costs for solar PV, onshore wind and offshore wind decreased by about 82%, 35% and 41%, respectively, and these positive trends will drop even further in the coming years (IRENA, 2022c). In addition, the investment cost and efficiency of electrolysers have shown remarkable improvements in recent years, which makes the cost of green hydrogen increasingly lower (Reksten et al., 2022).

1.2. Cost-optimal design of power-to-hydrogen systems

A cost-optimal design of power-to-hydrogen (PtH) systems – including the renewable energy generators and the electrolyser – is also fundamental to deliver green hydrogen at the lowest specific cost, as evidenced by the large number of recent studies on this topic. Hassan et al. (2023) conducted a thorough review of studies on green hydrogen production from a techno-economic, ecological and social perspective. Hofrichter et al. (2023) investigated the optimal ratio between the installed capacity of the electrolyser and the renewable energy generator (both PV and wind power plants). They considered off-grid renewable energy systems and computed levelised cost of hydrogen (LCOH) values as low as 2.5 €/kg. Scolaro and Kittner (2022) analysed the competitiveness of hydrogen production based on offshore wind farm in Germany. They found that the lowest LCOH occurs when the electrolyser capacity is 87% of the wind farm capacity and showed that participating in an ancillary service market can be economically beneficial. A wide range of LCOH values – from 6.2 to 57.6 €/kg – was derived in the work of Bhandari and Shah (2021), who investigated different PtH configurations (off-grid and grid-connected) considering both proton exchange membrane (PEM) and alkaline electrolysers. Tang et al. (2022) explored the economic competitiveness of PtH systems in Sweden and found that the LCOH ranges from 7.1 to 15.3 €/kg in off-grid scenarios and from 3.5 to 7.3 €/kg in on-grid scenarios. Gül and Akyüz (2023) investigated the technical and economic viability of photovoltaic-powered hydrogen production in Turkey and considered future cost projections up to 2050. They calculated a projected minimum hydrogen cost in the range of 1.4–3.0 $/kg for the year 2050. Scheepers et al. (2023) showed that the optimal design and operation of an electrolyser strongly depends on the framework conditions under which the operation takes place, such as electrolyser investment cost and electricity price. María Villarreal Vives et al. (2023) observed that the cost of electricity consumed for hydrogen production is generally the largest contributor to the LCOH. In particular, they evaluated the hydrogen cost under different electricity prices considering a 10-MW PEM electrolyser. The strong dependence of the LCOH on the electricity price was also reported by Superchi et al. (2023), who carried out a techno-economic analysis of wind-powered green hydrogen production for the decarbonisation of a steel mill.

1.3. Novelty and aim of the study

The analysis of the existing literature on PtH systems has revealed a gap that demands attention: many assessments are confined to specific case studies, without providing the generalisation of results needed for broader applicability across diverse scenarios. In particular, the literature currently lacks indicators for replication analysis and key insights into the profitability of PtH systems.

Within this context, the primary objective of this work is to derive an optimisation framework to address the optimal design of hydrogen production systems. To bridge the identified gap, the present study aims to:

- Establish a comprehensive set of indicators – encompassing technical, energy and environmental performance – that can be used to characterise PtH systems with a generalised approach, going beyond the analysis of specific case studies.
- Provide readers with guidelines for the optimal design of PtH systems under various conditions. Special emphasis is placed on investigating the impact of grid electricity price on the optimal design of hydrogen production systems.

In the present work, the model of the PtH system is based on a Mixed Integer Linear Programming (MILP) approach and includes an electrolyser, which is powered by local RES and grid electricity. A real efficiency curve of a MW-size PEM electrolyser is also implemented within the MILP-based framework to strengthen the accuracy of the PtH model. In order to match the variable RES production and the hydrogen demand, flexibility on the supply side can be provided through the integration of a battery electricity storage and a hydrogen storage.

The structure of this work is as follows: Section 2 shows the methodology for the optimal design of the PtH system along with the main techno-economic assumptions; results are presented and discussed in Section 3; finally the main conclusions are summarised in Section 4.

2. Methodology

Fig. 1 shows the layout of the PtH system studied in this work. The electrolyser is powered by electricity coming from an on-site solar PV system and/or the electrical grid. A hydrogen storage is included to reliably cover the hydrogen demand of the end-user. A battery storage can also be integrated to enhance the exploitation of the local solar resource. Finally, excess renewable power, if not stored, can be sold to the electrical grid to improve the profitability of the PtH business case.

The overall structure of the proposed methodology is illustrated in Fig. 2. A MILP-based optimisation framework (green box in Fig. 2) was formulated to address the optimal sizing and operation of the PtH system. The total net present cost (NPC) was selected as objective function of the optimisation problem. The description of the optimisation

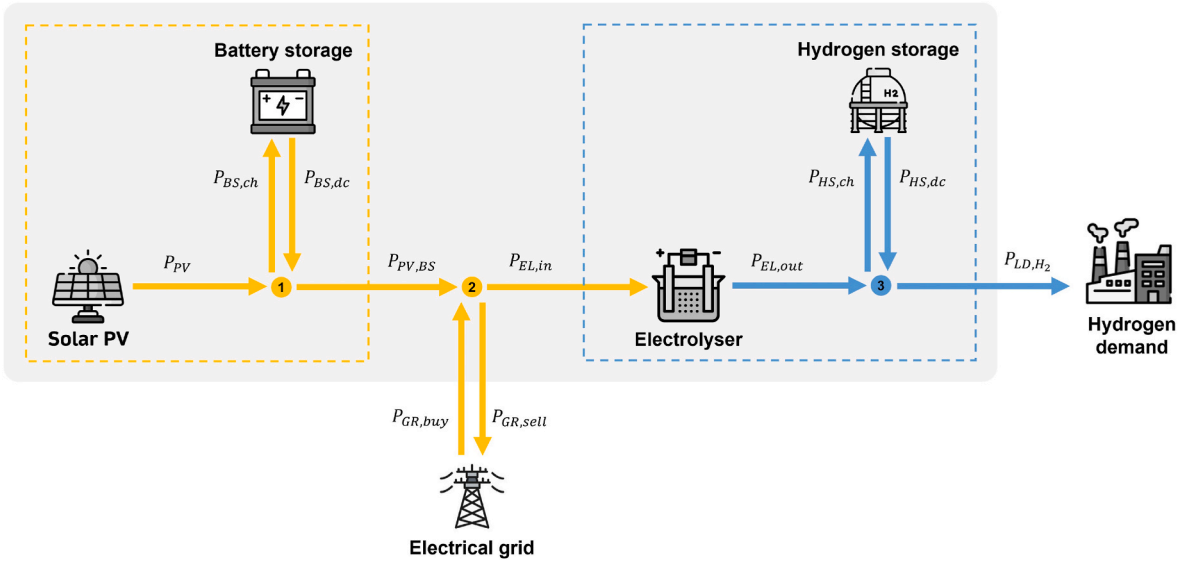

Fig. 1. Layout of the power-to-hydrogen system.

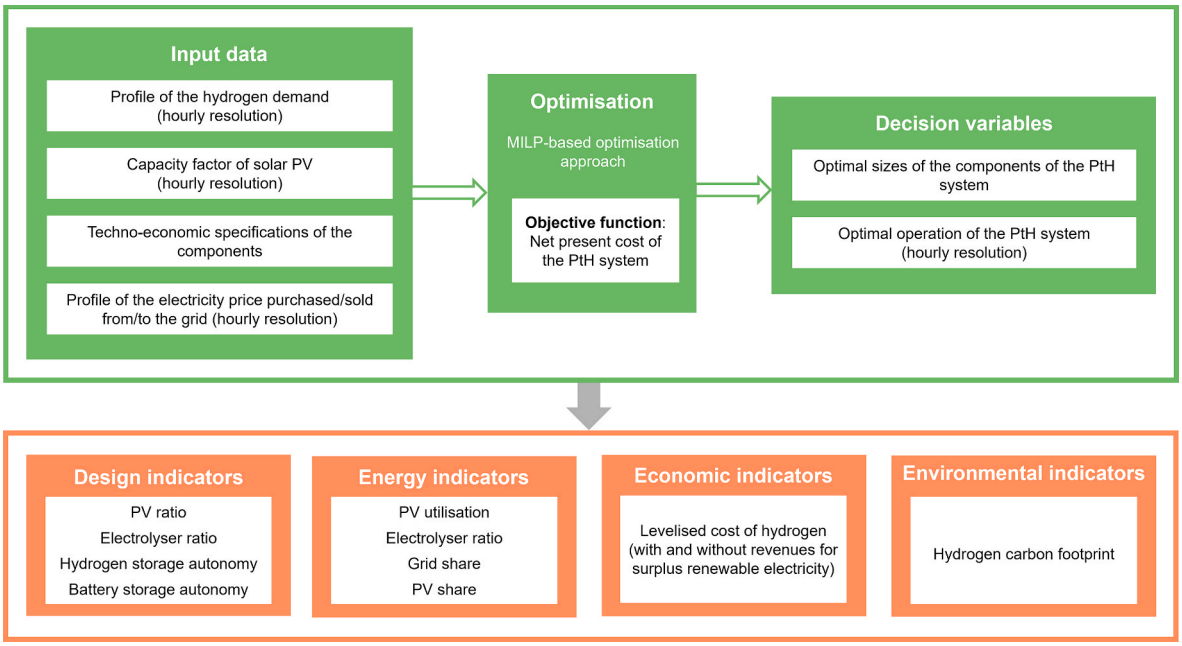

Fig. 2. Schematic of the methodology, which includes an optimisation framework for the optimal design of the power-to-hydrogen system (green box) and a post-processing stage for the evaluation of the indicators (red box).

framework is presented in Sections 2.1 to 2.5. The toll was implemented in Matlab® and the optimisation problem was solved using the Gurobi™ solver.

Building upon the outcomes of the optimisation process, a set of indicators was derived to evaluate the techno-economic and environmental performance of the PtH system (red box in Fig. 2). The definition of these indicators is depicted in Section 2.6.

2.1. Optimisation framework

The objective of the optimisation problem is to satisfy the hydrogen demand for each time step (t) of the time horizon (T) while minimising the net present cost of the PtH system. In particular, the simulation was conducted considering a year-long time horizon with hourly resolution. The choice of a 1-h time step represents a good compromise between the accuracy of the results and the computational burden (Das et al., 2021).

The main inputs to the MILP-based optimisation process are the following:

i. The hydrogen demand that must be covered $\forall\, t \in T$.
ii. The meteorological data on the RES availability, here implemented as power production (in terms of capacity factor) $\forall\, t \in T$
iii. The price of electricity purchased from the grid (electricity purchase price) and the price of electricity sold to the grid (electricity sale price) $\forall\, t \in T$
iv. The techno-economic data of all the components of the PtH system, i.e. solar photovoltaics (PV), battery storage (BS), electrolyser (EL) and hydrogen storage (HS).

The following decision variables are returned:

i. The sizes of all the components of the PtH system, i.e. PV, BS, EL and HS
ii. The on/off status of the electrolyser $\forall\, t \in T$
iii. The input power to the electrolyser (electricity) and the output power from the electrolyser (hydrogen) $\forall\, t \in T$
iv. The electrical power purchased from the grid and sold to the grid $\forall\, t \in T$
v. The charging and discharging power of the BS and HS $\forall\, t \in T$
vi. The amount of energy stored in the BS and HS $\forall\, t \in T$

Decision variables (i), namely the sizes of the installed PtH technologies, are denoted as design variables. Instead, decision variables (ii) to (vi) are referred to as operation variables and are computed for each time step (t) of the time horizon (T).

Based on the outcomes (i.e. decision variables) of the optimisation process, a post-processing routine was employed to calculate techno-economic and environmental indicators (see Section 2.6 for a complete list of all indicators).

The sizes (rated power) of the PV and EL components were treated as continuous variables, which were constrained between a minimum and maximum value as set out below (with j = PV, EL):

$$P_{j,rated,min} \leq P_{j,rated} \leq P_{j,rated,max} \tag{1}$$

where $P_{j,rated}$ is the rated power of the j-th component. The $P_{EL,rated}$ variable refers to the rated input power (electricity) of the electrolyser system.

Similarly, the sizes (rated energy) of the battery and hydrogen storage systems were constrained as follows (with j = BS, HS):

$$E_{j,rated,min} \leq E_{j,rated} \leq E_{j,rated,max} \tag{2}$$

where $E_{j,rated}$ is the rated energy of the j-th component. In Eqs. (1) and (2), the minimum size values were set to zero, meaning that a certain technology is installed in the PtH system if the optimisation process returns a value of its size greater than zero.

2.2. Power balances

As shown in Fig. 1, three different power balances must be satisfied for all time steps of the simulation period. The first power balance (electricity, in kW) refers to the PV-BS subsystem and was expressed as follows:

$$P_{PV}(t) + P_{BS,dc}(t) = P_{BS,ch}(t) + P_{PV,BS}(t) \tag{3}$$

where P_{PV} is the power generated on-site by the PV plant, $P_{BS,dc}$ is the discharging power of the battery storage, $P_{BS,ch}$ is the charging power of the battery storage and $P_{PV,BS}$ is the net power exiting the PV-BS subsystem. According to Eq. (3), as is common with solar PV plants, the battery is conceived as a support to maximise the on-site RES exploitation. At any time step, the PV power (P_{PV}) can be computed based on the capacity factor (CF) of the PV plant (CF_{PV}, in %). The latter is defined as the ratio of the electrical energy produced by the PV system over a given time step t to the theoretical maximum electrical energy generation over that period:

$$CF_{PV}(t) = \frac{P_{PV}(t) \cdot \Delta t}{P_{PV,rated} \cdot \Delta t} \tag{4}$$

where Δt (in h) is the duration of the time step and $P_{PV,rated}$ (in kW) is the PV rated power.

The second power balance (electricity, in kW), reported in Eq. (5), defines the interaction of the PtH system with the electrical grid. The electricity required by the electrolyser can be taken from the solar PV plant and/or the electrical grid. Moreover, the excess renewable power can be valorised by selling it to the grid.

$$P_{PV,BS}(t) + P_{GR,buy}(t) = P_{EL,in}(t) + P_{GR,sell}(t) \tag{5}$$

where $P_{GR,buy}$ is the power purchased from the electrical grid, $P_{GR,sell}$ is the power sold to the electrical grid and $P_{EL,in}$ is the input power to the electrolyser.

The third power balance (hydrogen, in kW) concerns the hydrogen production subsystem. It determines the electrolyser output power and the power exchanges with the hydrogen storage to cover the hydrogen demand of the end-user. This can be expressed as follows:

$$P_{EL,out}(t) + P_{HS,dc}(t) = P_{HS,ch}(t) + P_{LD,H_2}(t) \tag{6}$$

where $P_{EL,out}$ is the output power from the electrolyser, $P_{HS,dc}$ is the discharging power of the hydrogen storage, $P_{HS,ch}$ is the charging power of the hydrogen storage and P_{LD,H_2} is the hydrogen demand that must be covered (which is set as input to the problem).

2.3. Electrolyser

The modulation range of the electrolyser was defined according to the following expressions:

$$P_{EL,in}(t) \geq y_{EL,min} \cdot P_{EL,rated,aux}(t) \tag{7}$$

$$P_{EL,in}(t) \leq y_{EL,max} \cdot P_{EL,rated,aux}(t) \tag{8}$$

where $y_{EL,min}$ and $y_{EL,max}$ represent the lower and upper limits of the electrolyser modulation range (they are defined as a percentage of the electrolyser rated power). $P_{EL,rated,aux}$ is an auxiliary variable that was introduced to describe the product of the design variable $P_{EL,rated}$ (continuous) and the operation variable δ_{EL} (binary):

$$P_{EL,rated,aux}(t) = P_{EL,rated} \cdot \delta_{EL}(t) \tag{9}$$

where δ_{EL} is a binary variable that is equal to 1 if the electrolyser is on and 0 if the electrolyser is off. Eq. (9) can be linearised according to the following set of linear inequalities (Bemporad and Morari, 1999):

$$P_{EL,rated,aux}(t) \leq P_{EL,rated} - (1 - \delta_{EL}(t)) \cdot P_{EL,rated,min} \tag{10}$$

$$P_{EL,rated,aux}(t) \geq P_{EL,rated} - (1 - \delta_{EL}(t)) \cdot P_{EL,rated,max} \tag{11}$$

$$P_{EL,rated,aux}(t) \leq P_{EL,rated,max} \cdot \delta_{EL}(t) \tag{12}$$

$$P_{EL,rated,aux}(t) \geq P_{FC,rated,min} \cdot \delta_{EL}(t) \tag{13}$$

A partial-load performance curve was considered to model the electrolyser operation. For each point of the modulation range, the curve relates the electrolyser output power (hydrogen) to the electrolyser input power (electricity).

The performance curve was implemented within the MILP framework by means of a piecewise affine (PWA) approximation. According to the PWA approach, the performance curve – which is nonlinear – can be approximated by a series of linear segments (Gabrielli et al., 2018). The optimal position of the n breakpoints on the curve was determined by applying the nonlinear optimisation problem described in (Marocco et al., 2021). Then, for each i-th segment of the PWA approximation, the following expression was used to express the electrolyser output power ($P_{EL,out}$) based on the electrolyser input power ($P_{EL,in}$):

$$P_{EL,out}(t) \leq \alpha_i \cdot P_{EL,in}(t) + \beta_i \cdot P_{EL,rated,aux}(t) \tag{14}$$

where α_i and β_i are the coefficients of the i-th affine segment.

2.4. Energy storage technologies

At any time step, the amount of energy in the battery storage can be calculated on the basis of the energy stored in the previous time step and the battery operating power:

$$E_{BS}(t+1) = (1-\sigma_{BS})\cdot E_{BS}(t) + \eta_{BS,ch}\cdot P_{BS,ch}(t)\cdot\Delta t - \frac{P_{BS,dc}(t)\cdot\Delta t}{\eta_{BS,dc}} \quad (15)$$

where E_{BS} (in kWh) is the energy stored in the battery storage, σ_{BS} (in %/h) is the self-discharge coefficient of the battery storage (namely the energy losses expressed as a percentage of the rated energy in each time step), $\eta_{BS,ch}$ (in %) is the battery charging efficiency, $\eta_{BS,dc}$ (in %) is the battery discharging efficiency and Δt (in h) is the duration of the time step.

Analogously, the behaviour of the hydrogen storage technology was described by the following linear dynamics:

$$E_{HS}(t+1) = E_{HS}(t) + P_{HS,ch}(t)\cdot\Delta t - P_{HS,dc}(t)\cdot\Delta t \quad (16)$$

where E_{HS} (in kWh) is the energy stored in the hydrogen storage. It should be noted that, in contrast to the battery storage, the self-discharge coefficient does not appear in the energy balance of Eq. (16) since the self-discharge losses for the hydrogen storage are negligible.

Eqs. (17) and (18) were also introduced to constrain the amount of energy that can be stored (with j = BS, HS):

$$E_j(t) \geq E_{j,rated}\cdot y_{j,min} \quad (17)$$

$$E_j(t) \leq E_{j,rated}\cdot y_{j,max} \quad (18)$$

where $y_{j,min}$ and $y_{j,max}$ are the minimum and maximum state-of-charge (SOC) values of the j-th storage technology.

2.5. Objective function

The objective function of the optimisation problem is total net present cost (NPC) of the power-to-hydrogen system over its lifetime. The total NPC ($C_{NPC,tot}$, in €) includes capital (CAPEX) and operating (OPEX) expenditures:

$$C_{NPC,tot} = C_{NPC,capex,tot} + C_{NPC,opex,tot} \quad (19)$$

Specifically, the $C_{NPC,capex,tot}$ term – which takes place at year zero – was derived as the sum of the CAPEX of all technologies involved in the PtH system, i.e., PV generator, battery storage, electrolyser and hydrogen storage:

$$C_{NPC,capex,tot} = C_{capex,PV} + C_{capex,BS} + C_{capex,EL} + C_{capex,HS} \quad (20)$$

The $C_{NPC,opex,tot}$ term was instead computed according to the following expression (with j = PV, BS, EL, HS):

$$C_{NPC,opex,tot} = \sum_{n=1}^{N} \frac{\sum_j (C_{opex,j}) + C_{GR,buy}}{(1+d)^n} \quad (21)$$

where N (in years) is the project lifetime, $C_{opex,j}$ is the annual operating cost due to the j-th component, $C_{GR,buy}$ is the annual cost due to the electricity purchased from the grid and d (in %) is the discount rate. The $C_{opex,j}$ term was calculated as a fraction of the CAPEX of the j-th component. It also includes the replacement cost in case the j-th component must be replaced during the n-th year.

It is worth highlighting that the objective function ($C_{NPC,tot}$) does not include revenues from the sale of the excess PV energy. This exclusion is intended to prevent the PtH system from being oversized for the purpose of selling electricity to the grid (which is not the primary objective of a PtH system).

2.6. Indicators

Various indicators were introduced to provide general criteria for the design of the PtH system and to describe its techno-economic and environmental performance.

The energy and environmental indicators reported below were computed over the time horizon T, namely 1 year in this analysis. A summary of all indicators can be found in Table 1.

2.6.1. Design indicators

2.6.1.1. PV ratio. The PV ratio (R_{PV}) is defined as the ratio between the PV rated power and the electrolyser rated power:

$$R_{PV} = \frac{P_{PV,rated}}{P_{EL,rated}} \quad (22)$$

2.6.1.2. Electrolyser ratio. The electrolyser ratio (R_{EL}) gives an indication of the size of the electrolyser with respect to the average hydrogen load:

$$R_{EL} = \frac{P_{EL,rated}\cdot\eta_{EL,rated}}{P_{LD,H_2,avg}} \quad (23)$$

where $\eta_{EL,rated}$ (in %) is the efficiency of the electrolyser under rated conditions, and $P_{LD,H_2,avg}$ (in kW) is the average hydrogen load to be covered.

2.6.1.3. Hydrogen storage autonomy. The hydrogen storage autonomy (A_{HS}, in h) indicates the period of time during which the hydrogen storage is able to cover the average hydrogen demand. It can be defined as the ratio of the HS size to the average hydrogen demand:

$$A_{HS} = \frac{E_{HS,rated}}{P_{LD,H_2,avg}} \quad (24)$$

Table 1
List of indicators introduced for the analysis of the PtH system.

Indicator	Symbol	Unit	Description
Design indicators			
PV ratio	R_{PV}	-	Ratio of the PV rated power to the electrolyser rated power
Electrolyser ratio	R_{EL}	-	Ratio of the hydrogen production under rated conditions to the average hydrogen demand
Hydrogen storage autonomy	A_{HS}	h	Ratio of the hydrogen storage size to the average hydrogen demand*
Battery storage autonomy	A_{BS}	h	Ratio of the battery storage size to the electrolyser rated power
Energy indicators			
PV utilisation*	U_{PV}	%	Fraction of PV energy that is used by the electrolyser for hydrogen production
Electrolyser utilisation*	U_{EL}	%	Ratio of actual electrical energy used by the electrolyser to the maximum amount it could utilise
Grid share*	y_{GR}	%	Fraction of the electrical energy supplied to the electrolyser that comes from the electrical grid
PV share*	y_{PV}	%	Fraction of the electrical energy supplied to the electrolyser that comes from the on-site PV plant
Economic indicators			
Levelised cost of hydrogen	C_{H_2}	€/kg$_{H2}$	Average net present cost of hydrogen production over the project lifetime
Environmental indicators			
Hydrogen carbon footprint*	ε_{H_2}	kg$_{CO2,e}$/kg$_{H2}$	Average emissions intensity of hydrogen production

* calculated over the time horizon T, specifically 1 year in this analysis.

2.6.1.4. Battery storage autonomy. The battery storage autonomy (A_{BS}, in h) indicates how long the battery storage is able to cover the energy demand of the electrolyser under rated conditions. It is determined by the ratio of the battery storage size to the rated power of the electrolyser.

$$A_{BS} = \frac{E_{BS,rated}}{P_{EL,rated}} \tag{25}$$

It is worth noting that the autonomy of the battery storage is defined in relation to the load that the battery (rated capacity) is intended to satisfy, specifically the rated power of the electrolyser.

2.6.2. Energy indicators

2.6.2.1. PV utilisation. The PV utilisation (U_{PV}, in %) indicates the fraction of PV energy that is used by the electrolyser for hydrogen production (the remaining share of PV energy can be curtailed or sold to the grid). This indicator is thus defined from the perspective of a PtH business case.

$$U_{PV} = \frac{\sum_{t=1}^{T}\left(P_{EL,in}(t)\cdot\Delta t - P_{GR,buy}(t)\cdot\Delta t\right)}{\sum_{t=1}^{T}\left(P_{PV,BS}(t)\cdot\Delta t\right)} \tag{26}$$

2.6.2.2. Electrolyser utilisation. The electrolyser utilisation (U_{EL}, in %) measures the energy utilisation of the electrolyser compared to the maximum amount it could utilise without any interruption:

$$U_{EL} = \frac{\sum_{t=1}^{T}\left(P_{EL,in}(t)\cdot\Delta t\right)}{\sum_{t=1}^{T}\left(P_{EL,rated}\cdot\Delta t\right)} \tag{27}$$

2.6.2.3. Grid share. The grid share (y_{GR}, in %) represents the fraction of electrical energy consumed by the electrolyser that comes from the grid (the remainder is produced locally by the PV plant):

$$y_{GR} = \frac{\sum_{t=1}^{T}\left(P_{GR,buy}(t)\cdot\Delta t\right)}{\sum_{t=1}^{T}\left(P_{EL,in}(t)\cdot\Delta t\right)} \tag{28}$$

2.6.2.4. PV share. The PV share (y_{PV}, in %) represents the fraction of electrical energy consumed by the electrolyser that comes from the on-site PV plant. It can be computed based on the grid share as follows:

$$y_{PV} = 100\% - y_{GR} \tag{29}$$

2.6.3. Economic indicators

2.6.3.1. Levelised cost of hydrogen. The levelised cost of hydrogen (C_{H_2}, in €/kg) indicates the average net present cost of hydrogen production for a PtH system over its lifetime. It can be expressed according to the following expression:

$$C_{H_2} = \frac{C_{NPC,tot} - C_{GR,sell}}{\sum_{n=1}^{N}\frac{M_{H_2}}{(1+d)^n}} \tag{30}$$

where $C_{NPC,tot}$ is the NPC of the PtH system over its lifetime (computed according to Eq. (19)), $C_{GR,sell}$ is the annual revenue from selling excess electricity to the grid, and M_{H_2} (in kg/y) is the amount of hydrogen produced annually by the PtH system.

In Section 3, different values for the electricity sale price will be investigated, ranging from zero (scenario with no revenues associated with the surplus electricity) to higher values.

2.6.4. Environmental indicators

2.6.4.1. Hydrogen carbon footprint. The hydrogen carbon footprint (ε_{H_2}, in $kg_{CO2,e}/kg_{H2}$) indicates the kilogrammes of CO_2 equivalent ($CO_{2,e}$) emitted per kilogramme of hydrogen produced:

$$\varepsilon_{H_2} = \frac{\sum_{t=1}^{T}\left(P_{GR,buy}(t)\cdot\Delta t\cdot\varepsilon_{GR}\cdot 10^{-3}\right)}{\sum_{t=1}^{T}\left(P_{EL,out}(t)\cdot\Delta t\cdot\Delta h_{H_2}^{-1}\right)} \tag{31}$$

where ε_{GR} (in $g_{CO2,e}$/kWh) is the electricity carbon intensity (ECI), namely how many grams of $CO_{2,e}$ are released per kilowatt-hour of electricity withdrawn from the grid (it refers to the average energy mix of the selected country), and Δh_{H_2} (in kWh/kg_{H2}) is the lower heating value (LHV) of hydrogen.

2.7. Input data

The analysis was applied to Italy and a country-aggregated profile of the PV capacity factor was used for the estimation of the PV (fixed tilt) power production (according to Eq. (4)). The profile of the PV CF (Fig. 3) has an hourly resolution and was taken from (Pfenninger and Staffell, 2016): it refers to the year 2016, which was identified as the most-typical reference weather year for Italy (Lombardi et al., 2020).

Hydrogen is expected to play a key role in decarbonising those sectors that are hard to abate like cement, iron and steel, and chemicals production. The hydrogen request by heavy industry applications is usually constant over time, e.g., steelmaking process (Superchi et al., 2023) and ammonia production (IEA, 2021). In this work, the hydrogen demand was thus set constant to be representative of a typical industrial process.

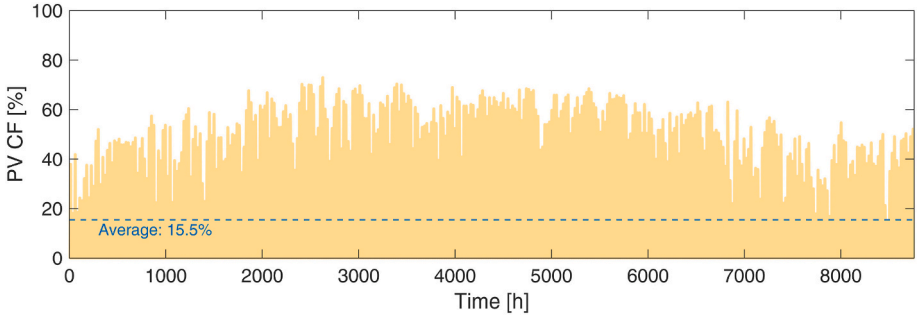

Fig. 3. Time series of the PV capacity factor over the reference year (2016) in Italy. The resulting annual average CF is 15.5%.

Table 2
Input data for the PtH system modelling.

	Value	Ref.
Photovoltaic		
CAPEX	650 €/kW	Danish Energy Agency (2022)
OPEX (annual)	2% (% of CAPEX)	Jamshidi and Askarzadeh (2019)
Lifetime	Project lifetime	
Battery storage (Li-ion)		
Charging efficiency	95%	Marocco et al. (2022)
Discharging efficiency	95%	Marocco et al. (2022)
SOC range	20%–100%	Marocco et al. (2022)
Self-discharge rate	0.007%/h	Marocco et al. (2022)
CAPEX (module + BOP)	306 €/kWh	Cole et al. (2021)
Replacement cost (module)	50% (% of CAPEX)	Marocco et al. (2022)
OPEX (annual)	2% (% of CAPEX)	Marocco et al. (2022)
Lifetime of the module	10 y	Marocco et al. (2022)
Lifetime of the BOP	Project lifetime	
Electrolyser (PEM)		
Minimum power	5% (% of rated power)	Patonia and Poudineh (2022)
Maximum power	100% (% of rated power)	
Efficiency	Efficiency curve (stack + BOP)	Eduardo and Maider (2021)
CAPEX (stack + BOP)	1188 €/kW	Marocco et al. (2023b)
Replacement cost (stack)	30% (% of CAPEX)	Tractebel (2017)
OPEX (annual)	3% (% of CAPEX)	
Lifetime of the stack	10 y	Marocco et al. (2023b)
Lifetime of the BOP	Project lifetime	
Hydrogen storage		
CAPEX	500 €/kg	Danish Energy Agency (2020)
OPEX (annual)	2% (% of CAPEX)	Marocco et al. (2023b)
Lifetime	Project lifetime	
Other assumptions		
Electricity purchase price	Sensitivity analysis (50–300 €/MWh)	
Electricity sale price[a]	40% of electricity purchase price (reference). Sensitivity analysis from 0% to 60% was also conducted.	(GME - Gestore dei Mercati Energetici SpA, 2023; Eurostat - Data Browser, 2022)
Discount rate	4%	Marocco et al. (2023b)
Project lifetime	20 y	Marocco et al. (2023b)
Electricity carbon intensity (ECI)	234 $g_{CO2,e}$/kWh (Italy, 2021) 238 $g_{CO2,e}$/kWh (EU-27, 2021) 114 $g_{CO2,e}$/kWh (EU-27, 2030)	European Environment Agency (2023)
Carbon footprint of renewable (or low-carbon) hydrogen[b]	<3 $kg_{CO2,e}/kg_{H2}$	(European Union, 2021; Ministero della Transizione Ecologica, 2022)

[a] The 40% value corresponds to the ratio between the electricity sale price on the market (Prezzo Unico Nazionale, PUN, sourced from GME for Italy (GME - Gestore dei Mercati Energetici SpA, 2023)) and the electricity purchase price. The evaluation was performed by averaging the electricity purchase price in different ranges of yearly consumption (obtained from Eurostat for Italy, (Eurostat - Data Browser, 2022)) for the period 2017–2020. The sensitivity analysis from 0% to 60% aims to cover all possible scenarios in terms of electricity sale price.

[b] 3 $kg_{CO2,e}/kg_{H2}$ is determined by applying the requirement for low-carbon gases to save at least 70% in terms of GHG emissions, according to the "Delegated regulation for a minimum threshold for GHG savings of recycled carbon fuels and annex" (1086/2023) (European Union, 2021).

The main techno-economic assumptions for the modelling of the PtH system are shown in Table 2.

A proton exchange membrane (PEM) electrolyser was considered for the production of hydrogen, as this technology is very suitable when coupled with variable RES (because of the good dynamic behaviour and wide modulation range) (Correa et al., 2022). A real efficiency curve of a MW-size PEM electrolysis system was used to enhance the robustness of the PtH model. Under rated conditions, the selected electrolyzer has an efficiency of 61% (LHV), while the maximum efficiency is 68% (LHV) and occurs at 20% of the rated power. These efficiency values are at system level and take into account the electrical consumption of both the stack and the balance-of-plant (BOP). The performance curve of the electrolyser was implemented within the MILP-based framework according to the PWA approximation described in Section 2.3. In this analysis, 5 breakpoints (corresponding to 4 linear segments) were used to approximate the performance curve, as this was found to provide an accurate description with a relative error always below 1.5% (in absolute value).

It should be noted that, in Table 2, the term "Electricity purchase price" refers to the price of electricity withdrawn from the grid and "Electricity sale price" represents the sale price of surplus PV electricity to the grid.

3. Results and discussion

For the sake of generalisation, the results are shown and discussed below by means of techno-economic and environmental indicators (previously defined in Section 2.6). The PtH system was designed with the aim of minimising the total NPC while meeting a constant hydrogen demand throughout the year.

3.1. Design and energy indicators

The electricity required by the electrolyser can be supplied by the on-site PV plant and/or the electrical grid. As shown in Fig. 4, the optimal values of the PV share and the grid share depend strongly on the purchase price of grid electricity. In scenarios with very low electricity prices (about 50 €/MWh), most of the electricity needed by the electrolyser – almost 80% – is provided by the grid. Then, this percentage value drops sharply when the electricity purchase price rises. From a cost-optimal point of view, when the price is higher than about 120 €/MWh, more than 80% of the electrical energy consumed by the electrolyser is generated on site by the PV plant. Therefore, the low CAPEX of PV technology currently makes it possible to rely heavily on the energy generated by the on-site PV system.

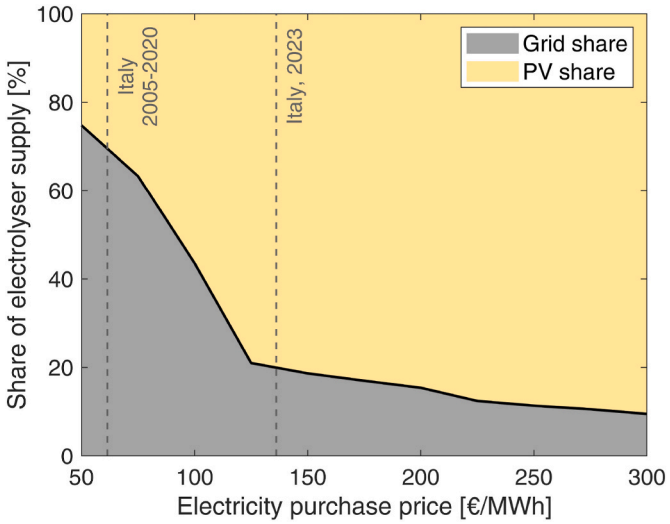

Fig. 4. Optimal values of grid share and PV share as a function of the electricity purchase price.

Fig. 5 shows the PV and EL indicators as a function of the electricity purchase price, which was varied from 50 €/MWh to 300 €/MWh.

The black dashed lines refer to a 100% PV-based configuration, i.e. no electricity is acquired from the grid to power the electrolyser. In this scenario, the optimal PV ratio is 3 (PV size is 3 times larger than the EL size), the EL ratio is 3.7 (hydrogen production under rated conditions is almost 4 times larger than the hydrogen demand), and the HS autonomy amounts to 120 h. A 100% PV-based system is therefore greatly oversized in order to always be able to cover the hydrogen demand without support from the electrical grid.

The red lines of Fig. 5 refer to configurations where electricity can be taken from the grid to power the hydrogen production process. At low electricity prices (about 50 €/MWh), the connection with the grid is strongly exploited and, consequently, both the PV and the electrolyser show utilisation factors close to 100%. Moreover, their sizes are at the minimum values within the analysed electricity price range: the EL ratio is 1 (the electrolyser works continuously under rated conditions to directly cover the hydrogen demand) and the PV ratio is 1.6. By increasing the electricity purchase price, the hydrogen production system moves towards a 100% PV-based configuration as it becomes progressively more convenient to rely on the PV plant. Indeed (see Fig. 5a), the optimal PV ratio rises from 1.6 (for an electricity price of 50 €/MWh) to 2.7 (for an electricity price of 300 €/MWh), which means that the PV plant becomes increasingly oversized to reliably meet the electrical demand of the electrolyser. As the PV ratio increases, the PV utilisation decreases from 100% to 76% (Fig. 5b) because of the higher amount of PV energy that is not exploited by the electrolyser for hydrogen production. Similar considerations also apply to the EL indicators: when changing from 50 €/MWh to 300 €/MWh, the optimal EL ratio increases from 1 to 2.8 (Fig. 5c) and the EL utilisation decreases from 100% to 35% (Fig. 5d). This occurs because the optimal EL size is oversized (with respect to the hydrogen demand) to cope with the variability in PV production (whose optimal share improves when moving to scenarios with higher electricity prices, as previously displayed in Fig. 4). These considerations align with the findings from Superchi et al. (2023), who

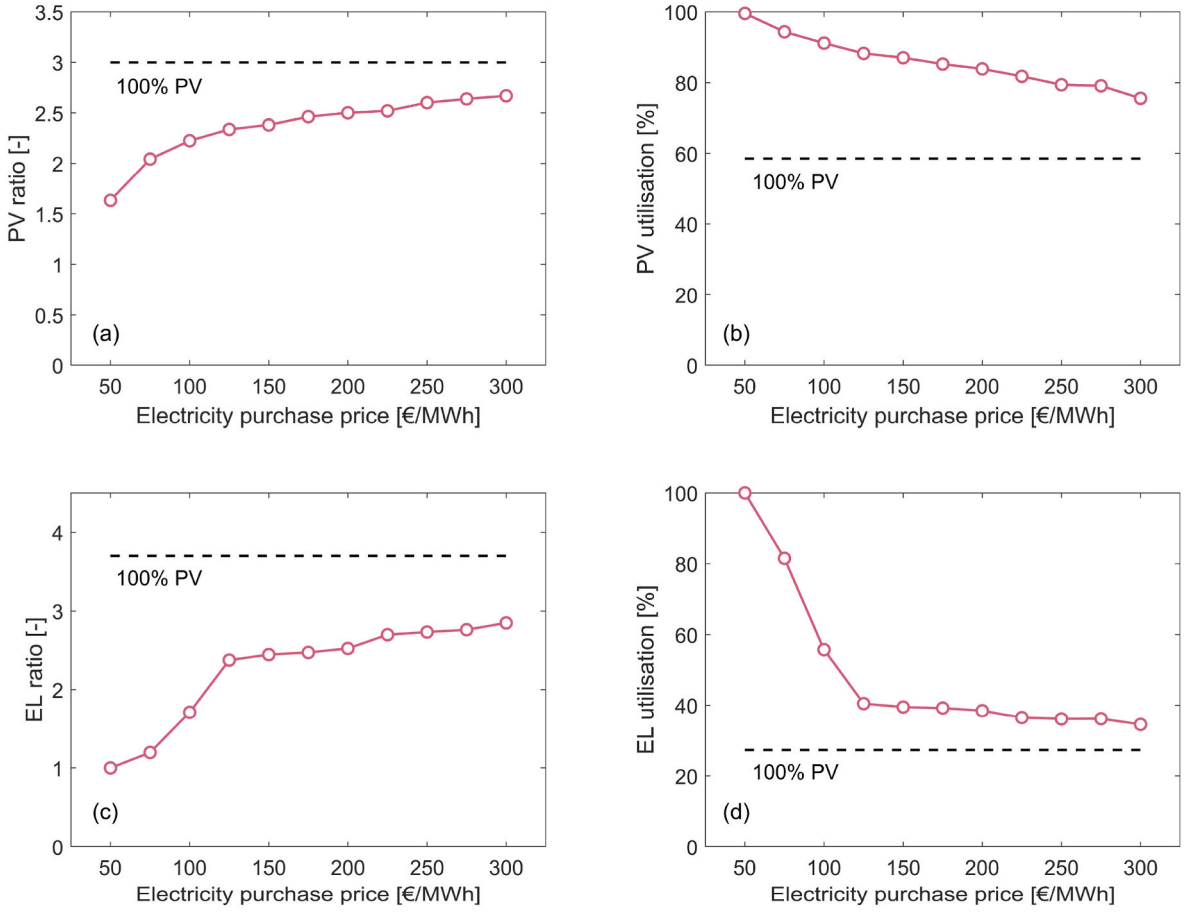

Fig. 5. PV ratio (a), PV utilisation (b), EL ratio (c) and EL utilisation (d) as a function of the electricity purchase price. The 100% PV-based solution is indicated by the black dashed lines.

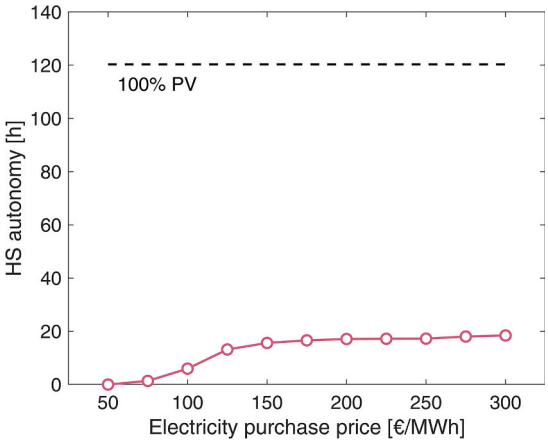

Fig. 6. Autonomy of the hydrogen storage as a function of the electricity purchase price. The HS autonomy of the 100% PV-based solution is around 120 h.

observed that increasing the rated power of the electrolyser and the renewable generator is advantageous as grid electricity prices rise.

The autonomy of the hydrogen storage as a function of the electricity purchase price is shown in Fig. 6 (red line). From a cost-optimal point of view, the HS autonomy enhances by increasing the purchase price of grid electricity. Specifically, at about 50 €/MWh, installing a hydrogen storage system is not cost-effective, while the optimal HS autonomy is up to 18 h for an electricity price of 300 €/MWh. Indeed, in scenarios with high electricity prices, the PtH system is encouraged to increase the share of energy from the PV system. A storage of hydrogen becomes thus necessary to balance the mismatch between PV generation and hydrogen demand, ensuring a reliable hydrogen supply to the end user over the entire year.

It should be observed that a maximum storage autonomy of about 18 h (with an electricity price of 300 €/MWh) is shown in Fig. 6 (red line), which corresponds to a PV share of approximately 90% (as depicted in Fig. 4). This value of HS autonomy is significantly lower than that observed in the 100% PV-based scenario (black dashed line), where it reaches 120 h. These findings underline the positive impact of the electrical grid integration on the overall design of the PtH system. Specifically, a grid share of only 10% leads to a substantial reduction in the HS autonomy from 120 to 18 h, thus enhancing the feasibility of the PtH system in terms of space and volume requirements.

It is also worth noting that the battery storage is never included in the optimal solution (i.e. the optimal value of the battery autonomy is always equal to zero), even in scenarios that are highly dependent on solar energy. From a cost-optimal perspective, it is therefore economically more advantageous to provide supply-side flexibility in the form of hydrogen storage rather than electricity storage. This outcome is further confirmed by the research by Garud et al. (2023), in which various sizes of hydrogen and battery storage were explored, highlighting that storing hydrogen molecules is cheaper than storing electrons. Superchi et al. (2023) also pointed out that the use of batteries only becomes economically viable when their price falls below 100 €/kWh, which is an optimistic value even in future scenarios (Cole et al., 2021).

3.2. Economic indicators

Fig. 7a shows the LCOH – and how it is distributed among the PtH components – for different values of the electricity purchase price. Two different scenarios were considered:

1. Scenario 1 (black-edge circles): There are no revenues for the excess renewable energy.
2. Scenario 2 (blue-edge triangles): The excess renewable energy is remunerated, and the electricity sale price is set equal to 40% of the electricity purchase price. The value of 40% was chosen since it is well representative for the annual average value of the ratio between the sale and purchase price of electricity in Italy (data from 2017 were analysed (GME - Gestore dei Mercati Energetici SpA, 2023; Eurostat - Data Browser, 2022)). Moreover, a sensitivity analysis on this percentage value (from 0% to 60%) was conducted to further investigate its impact on the LCOH. These additional results are shown in the Appendix.

In Scenario 1, with an electricity purchase price of 50 €/MWh, the LCOH amounts to 3.5 €/kg. Almost 60% of this cost is due to the electricity bought from the grid, whereas the remaining fraction is related to the PV plant (17%) and the electrolyser (25%). The LCOH progressively increases as the electricity purchase price rises, until reaching a cost of hydrogen of 7.0 €/kg at 300 €/MWh. This cost is mainly due to the PV and EL contributions, as also evidenced by the high values of PV and EL ratios (Fig. 5). The LCOH values of Scenario 2 are very similar to those of

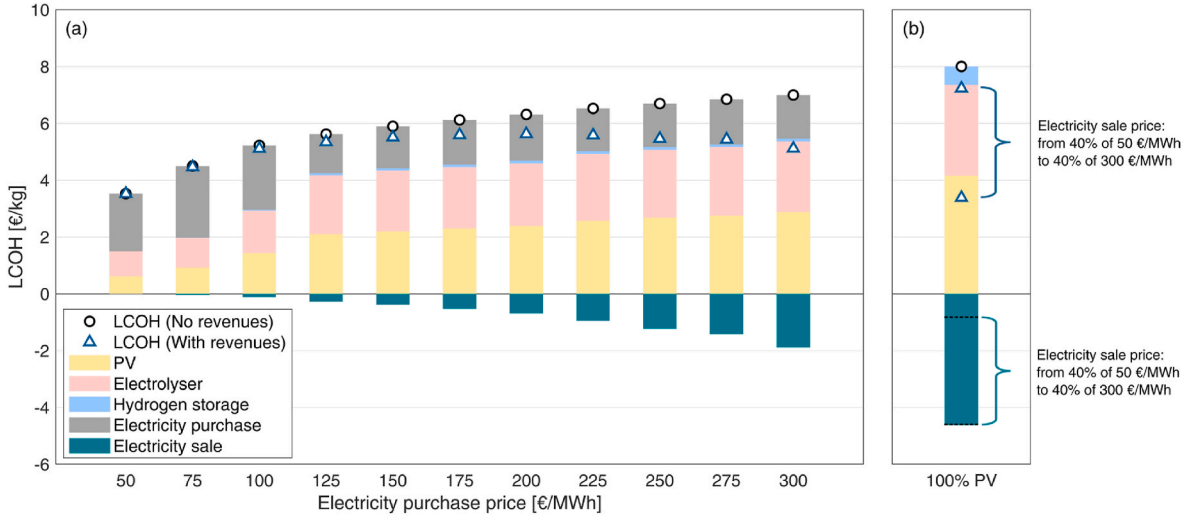

Fig. 7. a) LCOH as a function of the electricity purchase price (from 50 to 300 €/MWh), and b) LCOH for the 100% PV-based configuration. Two main scenarios are analysed: 1) no remuneration for the excess PV electricity (black-edge circles), and 2) the electricity sale price is set equal to 40% of the electricity purchase price (blue-edge triangles).

Scenario 1 up to about 100 €/MWh. Starting from this value, the revenues for the sale of excess electricity are no longer negligible (dark green areas) and cause the LCOH to decrease. Indeed, if the electricity purchase price rises, the optimal PV ratio also rises, which leads to an increase in the surplus PV energy. As an example, with a purchase price of 300 €/kWh, the LCOH is 7.0 €/kg in Scenario 1 (black-edge circle) and drops to 5.1 €/kg in Scenario 2 (blue-edge triangle).

As shown in Fig. 7b, Scenarios 1 and 2 were also applied to a 100% PV-based configuration, where no electricity is bought from the grid. In this specific case, Scenario 2 represents a PtH configuration where electricity cannot be drawn from the grid but can be fed into the grid (in the case of surplus PV energy). The LCOH of Scenario 1 amounts to 8.2 €/kg (black-edge circle), which is the highest LCOH value among all the configurations analysed. This high cost is due to a considerable oversizing of the PV plant (yellow area) and the electrolyser (pink area), as also depicted in Fig. 5 (black dashed lines). Regarding Scenario 2, a remuneration for the excess PV energy results in a reduction of the LCOH to 3.4–7.2 €/kg (blue-edge triangles) depending on the electricity sale price.

Finally, it is noteworthy that the cost of hydrogen storage (light-blue area) is quite negligible in almost all the configurations (Fig. 7a), except for the 100% PV-based case (Fig. 7b), where there is no electrical grid to limit the size of the hydrogen storage.

The range of hydrogen production costs determined in this study (from 3.4 to 8.2 €/kg) lies within the broad spectrum of production costs for PV-based PtH systems found in the literature. Hofrichter et al. (2023) evaluated the LCOH of PV-based hydrogen production systems at different geographical locations (with different solar potentials and PV capacity factors). They computed values in the range 3.1–5.9 €/kg for countries with high solar potential and 4.1–9.6 €/kg for those with low solar potential. Similar hydrogen production costs were also reported by Bhandari and Shah (2021), who collected several case studies from the literature about PEM-based PtH systems and found a median LCOH value of 5.1 €/kg.

3.3. Environmental indicators

Fig. 8 shows the hydrogen carbon footprint of the cost-optimal PtH system as a function of the electricity purchase price. Hydrogen can be defined as renewable (or low-carbon) if its carbon footprint is less than 3 $kg_{CO2,e}/kg_{H2}$ (European Union, 2021; Ministero della Transizione Ecologica, 2022). From an environmental perspective, the electrical grid is

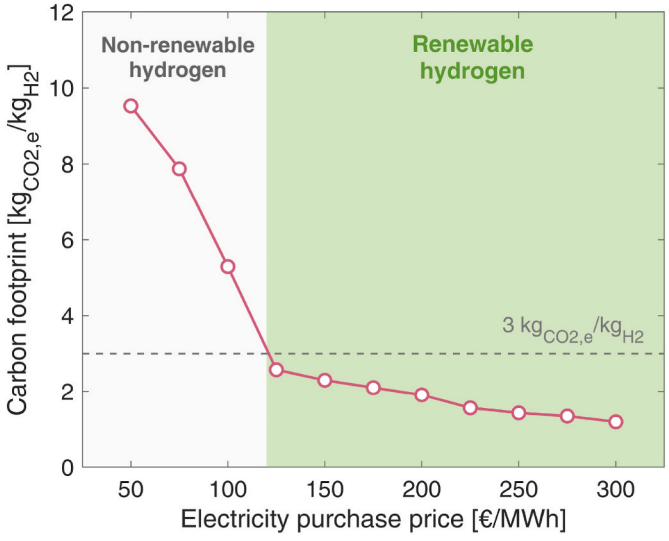

Fig. 8. Hydrogen carbon footprint as a function of the electricity purchase price. The electricity carbon intensity is 234 $g_{CO2,e}$/kWh (Italy, year 2021).

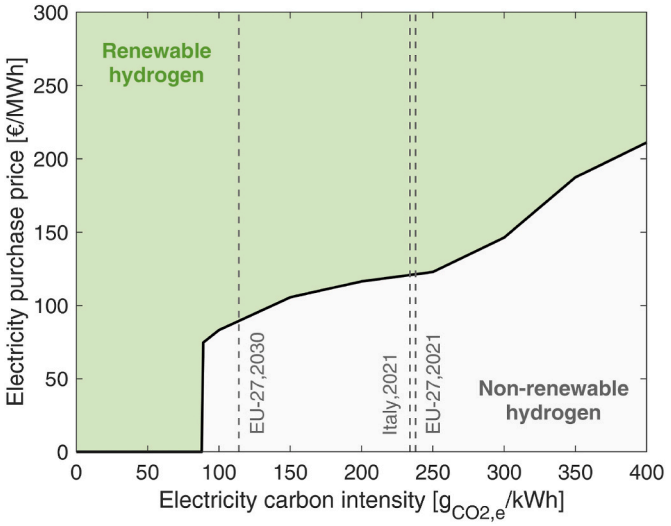

Fig. 9. Electricity purchase prices for which the cost-optimal design of the PtH system leads to the production of renewable (green area) or non-renewable (grey area) hydrogen. A sensitivity analysis on the electricity carbon intensity is conducted.

responsible for indirect GHG emissions, which depend on the energy production mix of a given country. It is here considered the average emission intensity of electricity generation in Italy for the year 2021 (i.e. 234 $g_{CO2,e}$/kWh (European Environment Agency, 2023)). The carbon footprint of hydrogen thus depends on how much electricity is taken from the grid to power the hydrogen production process. Consequently, the carbon footprint of hydrogen shows a decreasing trend as the price of electricity increases, similarly to what was previously observed for the optimal grid share (Fig. 4). It should be noted that, when considering an ECI of 234 $g_{CO2,e}$/kWh, cost-optimal solutions that involve the production of renewable hydrogen are found for electricity prices higher than 120 €/MWh (which corresponds to a grid share of less than about 20%).

By repeating this process for different values of electricity carbon intensity, a cost-optimal map (Fig. 9) was derived: for a given value of ECI (from 0 to 400 $g_{CO2,e}$/kWh), it shows the values of electricity purchase price for which the cost-optimal design of the PtH system leads to the production of renewable (green area) or non-renewable (grey area) hydrogen. Overall, considering current and future expected ECI values in Europe, the production of low-carbon hydrogen proves to be the most cost-effective solution in scenarios with prices of grid electricity above 100–120 €/MWh.

4. Conclusions

A MILP-based optimisation framework has been developed to address the optimal sizing and operation of PtH systems powered by an on-site PV plant and the electrical grid. The PtH system was designed to minimise the overall net present cost while satisfying a constant hydrogen demand over the entire year. The simulation was conducted considering a year-long time horizon with hourly resolution. For the purpose of generalisation, a set of techno-economic and environmental indicators was also introduced. The analysis was applied to Italy as a showcase and the main findings can be wrapped up as follows:

- The purchase price of grid electricity has a relevant influence on the optimal design of PV-based PtH systems. Overall, in scenarios with high electricity prices, it becomes economically advantageous to greatly oversize the PtH system, which tends to favour the use of fluctuating PV energy over the electrical grid. The PV ratio increases from 1.6 to 2.7 when the electricity price is varied from 50 to 300 €/MWh. The EL ratio rises as

well, from 1 to 2.8. The system oversizing also causes an increase in the excess renewable energy (i.e. the energy from on-site RES that is not exploited by the electrolyser).

- The optimal autonomy of hydrogen storage is in the range of 0–20 h when the electricity purchase price is between 50 and 300 €/MWh. Storage autonomy increases sharply, up to about 120 h, when considering a 100% PV-based configuration. The electrical grid – even in scenarios where it is poorly used – is thus essential to limit the size of the hydrogen storage.
- When addressing the optimal design of a PV-based hydrogen production system, it is more convenient to provide the supply-side flexibility in the form of hydrogen storage rather than electricity storage.
- The LCOH ranges between 3.5 and 7 €/kg, depending on the purchase price of grid electricity, and increases to 8.2 €/kg for an off-grid PtH configuration. The contribution of the hydrogen storage cost is almost negligible, except in the off-grid case, where it accounts for about 8% of the total LCOH. An LCOH reduction can be achieved if the excess renewable energy is remunerated, e.g. by selling it to the grid.
- The carbon footprint of hydrogen depends on the fraction of electricity purchased from the grid to supply the electrolyser. Given the current carbon intensity of grid electricity in Italy (234 $g_{CO2,e}$/kWh), the production of renewable hydrogen (i.e., carbon footprint of less than 3 $kg_{CO2,e}/kg_{H2}$) is the most cost-effective solution in scenarios with an electricity purchase price higher than 120 €/MWh (corresponding to grid share lower than 20%). Similar considerations apply when considering the average electricity carbon intensity of EU-27.

Based on the methodology derived in this study, future works will further explore the economic and environmental feasibility of RES-based PtH systems. In particular, the effect of hybridising the renewable energy generation system with both solar and wind energy will be investigated. The impact of the RES availability (i.e. capacity factor) will be also analysed by taking into account different geographical locations.

CRediT authorship contribution statement

Paolo Marocco: Conceptualization, Data curation, Formal analysis, Investigation, Methodology, Resources, Software, Validation, Visualization, Writing – original draft, Writing – review & editing. **Marta Gandiglio:** Conceptualization, Data curation, Formal analysis, Investigation, Resources, Visualization, Writing – review & editing. **Massimo Santarelli:** Project administration, Supervision, Writing – review & editing.

Declaration of competing interest

The authors declare that they have no known competing financial interests or personal relationships that could have appeared to influence the work reported in this paper.

Data availability

Data will be made available on request.

Acknowledgement

This publication is part of the project NODES which has received funding from the MUR – M4C2 1.5 of PNRR funded by the European Union - NextGenerationEU (Grant agreement no. ECS00000036).

Appendix

The impact of the electricity sale price on the LCOH is shown in Figure A1. Specifically, the electricity sale price was varied from 0% to 60% of the electricity purchase price. It can be seen that the influence of the sale price becomes increasingly significant as the purchase price increases. This is because, at high electricity purchase prices, the optimal PtH configuration results in greater quantities of excess PV energy.

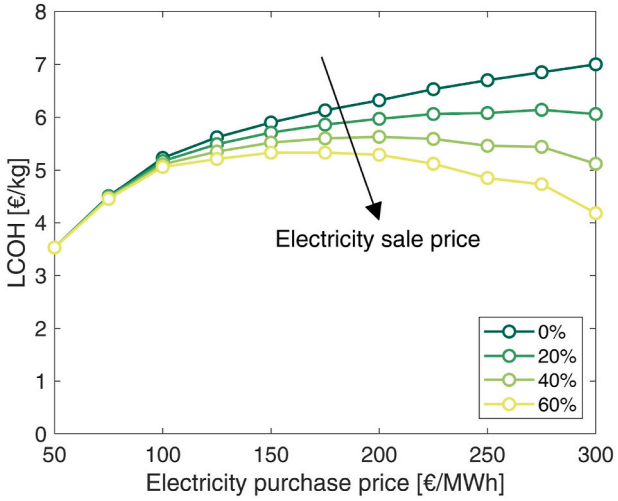

Fig. A1. LCOH (with revenues) as a function of the electricity purchase price. The electricity sale price was varied between 0% and 60% of the electricity purchase price.

Acronyms

BF-BOF	Blast Furnace-Basic Oxygen Furnace
BOP	Balance of plant
BS	Battery storage
CAPEX	Capital expenditures
CF	Capacity factor
DRI	Direct reduced iron
ECI	Electricity carbon intensity
EL	Electrolyser
GHG	Greenhouse gas
GR	Grid
HS	Hydrogen storage
LCOH	Levelised cost of hydrogen
LHV	Lower heating value
NPC	Net present cost
OPEX	Operating expenditures
PtH	Power-to-hydrogen
PV	Photovoltaic
RES	Renewable energy sources
SOC	State of charge

References

Bemporad, A., Morari, M., 1999. Control of systems integrating logic, dynamics, and constraints. Automatica 35, 407–427. https://doi.org/10.1016/S0005-1098(98)00178-2.

Bhandari, R., Shah, R.R., 2021. Hydrogen as energy carrier: techno-economic assessment of decentralized hydrogen production in Germany. Renew. Energy 177, 915–931. https://doi.org/10.1016/j.renene.2021.05.149.

Bionaz, D., Marocco, P., Ferrero, D., Sundseth, K., Santarelli, M., 2022. Life cycle environmental analysis of a hydrogen-based energy storage system for remote applications. Energy Rep. 8, 5080–5092. https://doi.org/10.1016/j.egyr.2022.03.181.

Cole, W., Frazier, A.W., Augustine, C., 2021. Cost Projections for Utility-Scale Battery Storage: 2021 Update, Golden, CO. https://www.nrel.gov/docs/fy21osti/79236.pdf. (Accessed 31 October 2023).

Correa, G., Marocco, P., Muñoz, P., Falagüerra, T., Ferrero, D., Santarelli, M., 2022. Pressurized PEM water electrolysis: dynamic modelling focusing on the cathode side. Int. J. Hydrogen Energy 47, 4315–4327. https://doi.org/10.1016/j.ijhydene.2021.11.097.

Danish Energy Agency, 2020. Energinet, Technology Data - Energy Storage. https://ens.dk/en/our-services/projections-and-models/technology-data/technology-data-energy-storage. (Accessed 10 April 2023).

Danish Energy Agency, 2022. Energinet, Technology Data. Generation of Electricity and District Heating. https://ens.dk/sites/ens.dk/files/Analyser/technology_data_catalogue_for_el_and_dh.pdf. (Accessed 31 October 2023).

Das, B.K., Hasan, M., Das, P., 2021. Impact of storage technologies, temporal resolution, and PV tracking on stand-alone hybrid renewable energy for an Australian remote area application. Renew. Energy 173, 362–380. https://doi.org/10.1016/j.renene.2021.03.131.

Eduardo, G., Maider, S., 2021. Protocols for Demonstration of Fuel-Production Strategy. Haeolus Project. Deliverable 8.3. https://www.haeolus.eu/?p=1073.

European Environment Agency, 2023. Greenhouse Gas Emission Intensity of Electricity Generation. https://www.eea.europa.eu/data-and-maps/daviz/co2-emission-intensity-13/#tab-chart_4. (Accessed 10 September 2023).

European Union, 2021. Regulation (EU) 2021/2139 of 4 June 2021. https://eur-lex.europa.eu/legal-content/EN/TXT/?uri=CELEX%3A02021R2139-20230101. (Accessed 31 October 2023).

Eurostat - Data Browser, 2022. Electricity Prices for Non-household Consumers - Bi-annual Data (From 2007 Onwards). https://ec.europa.eu/eurostat/databrowser/view/nrg_pc_204/default/table?lang=en. (Accessed 17 March 2023).

Gabrielli, P., Gazzani, M., Mazzotti, M., 2018. Electrochemical conversion technologies for optimal design of decentralized multi-energy systems: modeling framework and technology assessment. Appl. Energy 221, 557–575. https://doi.org/10.1016/j.apenergy.2018.03.149.

Gandiglio, M., Marocco, P., Bianco, I., Lovera, D., Blengini, G.A., Santarelli, M., 2022. Life cycle assessment of a renewable energy system with hydrogen-battery storage for a remote off-grid community. Int. J. Hydrogen Energy 47, 32822–32834. https://doi.org/10.1016/j.ijhydene.2022.07.199.

Garud, S.S., Tsang, F., Karimi, I.A., Farooq, S., 2023. Green hydrogen from solar power for decarbonization: what will it cost? Energy Convers. Manag. 286, 117059 https://doi.org/10.1016/j.enconman.2023.117059.

Genovese, M., Cigolotti, V., Jannelli, E., Fragiacomo, P., 2023. Current standards and configurations for the permitting and operation of hydrogen refueling stations. Int. J. Hydrogen Energy 1–15. https://doi.org/10.1016/j.ijhydene.2023.01.324.

GME - Gestore dei Mercati Energetici SpA, 2023. Esiti dei mercati e statistiche - Statistiche - Dati storici Excel. https://www.mercatoelettrico.org/it/. (Accessed 15 June 2023).

Gül, M., Akyüz, E., 2023. Techno-economic viability and future price projections of photovoltaic-powered green hydrogen production in strategic regions of Turkey. J. Clean. Prod., 139627 https://doi.org/10.1016/j.jclepro.2023.139627.

Hassan, Q., Abdulateef, A.M., Hafedh, S.A., Al-samari, A., Abdulateef, J., Sameen, A.Z., Salman, H.M., Al-Jiboory, A.K., Wieteska, S., Jaszczur, M., 2023. Renewable energy-to-green hydrogen: a review of main resources routes, processes and evaluation. Int. J. Hydrogen Energy 48, 17383–17408. https://doi.org/10.1016/j.ijhydene.2023.01.175.

Hofrichter, A., Rank, D., Heberl, M., Sterner, M., 2023. Determination of the optimal power ratio between electrolysis and renewable energy to investigate the effects on the hydrogen production costs. Int. J. Hydrogen Energy 48, 1651–1663. https://doi.org/10.1016/J.IJHYDENE.2022.09.263.

IEA, 2021. Ammonia Technology Roadmap: towards More Sustainable Nitrogen Fertiliser Production, Paris. https://www.iea.org/reports/ammonia-technology-roadmap. (Accessed 31 October 2023).

IEA, Global, 2022. Hydrogen Review 2022. https://www.iea.org/reports/global-hydrogen-review-2022. (Accessed 31 October 2023).

IRENA, 2018. Hydrogen from Renewble Power: Technology Outlook for the Energy Transition, Abu Dhabi. https://www.irena.org/publications/2018/sep/hydrogen-from-renewable-power. (Accessed 11 October 2023).

IRENA, 2021. Making the Breakthrough: Green Hydrogen Policies and Technology Costs, Abu Dhabi. https://www.irena.org/-/media/Files/IRENA/Agency/Publication/2020/Nov/IRENA_Green_Hydrogen_breakthrough_2021.pdf?la=en&hash=40FA5B8AD7AB1666EECBDE30EF458C45EE5A0AA6. (Accessed 31 October 2023).

IRENA, 2022a. Green Hydrogen for Industry. A Guide to Policy Making, Abu Dhabi. https://www.irena.org/publications/2022/Mar/Green-Hydrogen-for-Industry. (Accessed 31 October 2023).

IRENA, 2022b. Global Hydrogen Trade to Meet the 1.5°C Climate Goal. Part 1: Trade Outlook for 2050 and Way Forward, Abu Dhabi. https://www.irena.org/-/media/Files/IRENA/Agency/Publication/2022/Jul/IRENA_Global_hydrogen_trade_part_1_2022_.pdf. (Accessed 31 October 2023).

IRENA, 2022c. Renewable Power Generation Costs in 2021. https://www.irena.org/publications/2022/Jul/Renewable-Power-Generation-Costs-in-2021. (Accessed 31 October 2023).

Jamshidi, M., Askarzadeh, A., 2019. Techno-economic analysis and size optimization of an off-grid hybrid photovoltaic, fuel cell and diesel generator system. Sustain. Cities Soc. 44, 310–320. https://doi.org/10.1016/j.scs.2018.10.021.

Lombardi, F., Pickering, B., Colombo, E., Pfenninger, S., 2020. Policy decision support for renewables deployment through spatially explicit practically optimal alternatives. Joule 4, 2185–2207. https://doi.org/10.1016/j.joule.2020.08.002.

María Villarreal Vives, A., Wang, R., Roy, S., Smallbone, A., 2023. Techno-economic analysis of large-scale green hydrogen production and storage. Appl. Energy 346, 121333. https://doi.org/10.1016/j.apenergy.2023.121333.

Marocco, P., Ferrero, D., Martelli, E., Santarelli, M., Lanzini, A., 2021. An MILP approach for the optimal design of renewable battery-hydrogen energy systems for off-grid insular communities. Energy Convers. Manag. 245, 114564 https://doi.org/10.1016/J.ENCONMAN.2021.114564.

Marocco, P., Gandiglio, M., Santarelli, M., 2022. When SOFC-based cogeneration systems become convenient? A cost-optimal analysis. Energy Rep. 8, 8709–8721. https://doi.org/10.1016/j.egyr.2022.06.015.

Marocco, P., Novo, R., Lanzini, A., Mattiazzo, G., Santarelli, M., 2023a. Towards 100% renewable energy systems: the role of hydrogen and batteries. J. Energy Storage 57, 106306. https://doi.org/10.1016/J.EST.2022.106306.

Marocco, P., Gandiglio, M., Audisio, D., Santarelli, M., 2023b. Assessment of the role of hydrogen to produce high-temperature heat in the steel industry. J. Clean. Prod. 388, 135969 https://doi.org/10.1016/j.jclepro.2023.135969.

Massaro, M.C., Biga, R., Kolisnichenko, A., Marocco, P., Monteverde, A.H.A., Santarelli, M., 2023. Potential and technical challenges of on-board hydrogen storage technologies coupled with fuel cell systems for aircraft electrification. J. Power Sources 555, 232397. https://doi.org/10.1016/j.jpowsour.2022.232397.

Mertens, J., Breyer, C., Arning, K., Bardow, A., Belmans, R., Dibenedetto, A., Erkman, S., Gripekoven, J., Léonard, G., Nizou, S., Pant, D., Reis-Machado, A.S., Styring, P., Vente, J., Webber, M., Sapart, C.J., 2023. Carbon capture and utilization: more than hiding CO2 for some time. Joule 7, 442–449. https://doi.org/10.1016/j.joule.2023.01.005.

Ministero della Transizione Ecologica, 2022. Decreto 21 Settembre 2022. https://www.gazzettaufficiale.it/eli/id/2022/09/23/22A05525/sg. (Accessed 31 October 2023).

Patonia, A., Poudineh, R., 2022. Cost-competitive Green Hydrogen: How to Lower the Cost of Electrolysers? https://www.oxfordenergy.org/wpcms/wp-content/uploads/2022/01/Cost-competitive-green-hydrogen-how-to-lower-the-cost-of-electrolysers-EL47.pdf.

Pfenninger, S., Staffell, I., 2016. Long-term patterns of European PV output using 30 years of validated hourly reanalysis and satellite data. Energy 114, 1251–1265. https://doi.org/10.1016/j.energy.2016.08.060.

Reksten, A.H., Thomassen, M.S., Møller-Holst, S., Sundseth, K., 2022. Projecting the future cost of PEM and alkaline water electrolysers; a CAPEX model including electrolyser plant size and technology development. Int. J. Hydrogen Energy 47, 38106–38113. https://doi.org/10.1016/j.ijhydene.2022.08.306.

Scheepers, F., Stähler, M., Stähler, A., Müller, M., Lehnert, W., 2023. Cost-optimized design point and operating strategy of polymer electrolyte membrane electrolyzers. Int. J. Hydrogen Energy 8. https://doi.org/10.1016/j.ijhydene.2022.11.288.

Scolaro, M., Kittner, N., 2022. Optimizing hybrid offshore wind farms for cost-competitive hydrogen production in Germany. Int. J. Hydrogen Energy 47, 6478–6493. https://doi.org/10.1016/J.IJHYDENE.2021.12.062.

Superchi, F., Mati, A., Carcasci, C., Bianchini, A., 2023. Techno-economic analysis of wind-powered green hydrogen production to facilitate the decarbonization of hard-to-abate sectors: a case study on steelmaking. Appl. Energy 342, 121198. https://doi.org/10.1016/j.apenergy.2023.121198.

Tang, O., Rehme, J., Cerin, P., 2022. Levelized cost of hydrogen for refueling stations with solar PV and wind in Sweden: on-grid or off-grid? Energy 241, 122906. https://doi.org/10.1016/j.energy.2021.122906.

Tractebel, Hinicio, 2017. Study on Early Business Cases for H2 in Energy Storage and More Broadly Power to H2 Applications. https://hsweb.hs.uni-hamburg.de/projects/star-formation/hydrogen/P2H_Full_Study_FCHJU.pdf. (Accessed 31 October 2023).

van der Spek, M., Banet, C., Bauer, C., Gabrielli, P., Goldthorpe, W., Mazzotti, M., Munkejord, S.T., Røkke, N.A., Shah, N., Sunny, N., Sutter, D., Trusler, J.M., Gazzani, M., 2022. Perspective on the hydrogen economy as a pathway to reach net-zero CO2 emissions in Europe. Energy Environ. Sci. 15, 1034–1077. https://doi.org/10.1039/d1ee02118d.

Zainal, B.S., Ker, P.J., Mohamed, H., Ong, H.C., Fattah, I.M.R., Rahman, S.M.A., Nghiem, L.D., Mahlia, T.M.I., 2023. Recent advancement and assessment of green hydrogen production technologies. Renew. Sustain. Energy Rev. 189, 113941 https://doi.org/10.1016/j.rser.2023.113941.